Title: Highly effective methylated Ti MCM-41 catalyst for cyclohexene oxidation

Authors: Sushanta Kumar Roy, Debajani Dutta, Anup K. Talukdar

PII: S0025-5408(17)33038-6
DOI: https://doi.org/10.1016/j.materresbull.2018.03.017
Reference: MRB 9898

To appear in: *MRB*

Received date: 4-8-2017
Revised date: 1-1-2018
Accepted date: 9-3-2018

Please cite this article as: Roy SK, Dutta D, Talukdar AK, Highly effective methylated Ti MCM-41 catalyst for cyclohexene oxidation, *Materials Research Bulletin* (2010), https://doi.org/10.1016/j.materresbull.2018.03.017

Highly effective methylated Ti MCM-41 catalyst for cyclohexene oxidation

*Sushanta Kumar Roy, Debajani Dutta and Anup K. Talukdar**

Department of Chemistry, Gauhati University, Guwahati -781014, Assam, India

guchem.talukdar@gmail.com, roy16sushanta@gmail.com

Graphical Abstract:

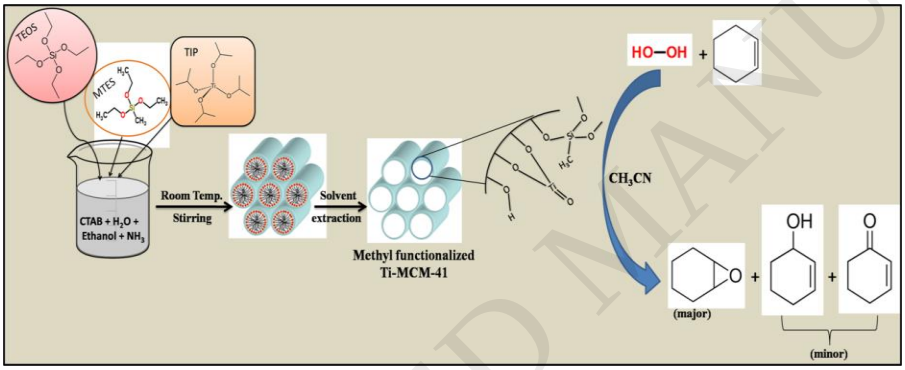

Highlights

- Methyl functionalized (methylated)TiMCM-41 materials are synthesized by the directroom temperature stirring in 3 h duration of time. In literature, no method was found using NH_3 as a base for the synthesis of methylated TiMCM-41.
- The synthesized materials are tested for theoxidationreaction of cyclohexene in the presence of H_2O_2 as an oxidant.
- Methylation improved the hydrophobicity of the catalytic active sites of TiMCM-41 materials.

Abstract:

A series of Ti containing MCM-41 materials were synthesized with different Si/Ti molar ratios and tested for cyclohexene epoxidation reaction. TiMCM-41 with Si/Ti ratio 40 which gave maximum conversion and selectivity to epoxide was methylated with methyltriethoxysilane (MTES) in this reaction. Accordingly, four different methyl loading (5, 10, 15 and 20 mol % of MTES w.r.t. TEOS) TiMCM-41(Si/Ti 40) samples were prepared. The materials were characterized by different physical techniques such as PXRD, FT-IR spectroscopy, UV-Vis DRS spectroscopy, N_2 adsorption-desorption isotherm, SEM-EDX, TEM, TGA and ICP-OES. The catalysts were then tested for cyclohexene epoxidation reaction in the presence of H_2O_2 avoiding TBHP. The conversion and selectivity for cyclohexene obtained with 10MeTiM-1 (Si/Ti 40) were found to be the best not only among the catalysts investigated in the present work, but also among all the catalysts studied so far for the reaction.

Keywords: TiMCM-41, Organofunctionalization, Cyclohexene, Epoxidation

1. Introduction:

Epoxidation of cyclohexene is an industrially important reaction as the product obtained has lots of synthetic application. Cyclohexene epoxide is used as monomer for the production of polycarbonate polymers [1]. Over the last few decades, titanium silicates have been used for catalyzing various oxidation reactions of hydrocarbons. Microporous TS-1[2], for example, has been attracting a great attention for its catalytic performance for selective oxidation of various organic substrates [3–9]. However, the microporous crystalline materials cannot catalyze conversion of bulky substrates, which are debared from accessing the active sites located inside the micropore (0.7 nm). The discovery of ordered mesoporous materials by Mobil Oil research group in 1992 promised to overcome this limitation and offered an opportunity to use these materials as catalyst [10-14]. The most important properties of these mesoporous materials are their large surface area allowing effective dispersion of catalytically active sites and large and tunable pore networks in the mesopore range, which help diffusion of comparatively larger

molecules. In addition, these materials have large pore volume and good thermal stability (within reaction temperature) and the surface can be readily modified. MCM-41, one of the members of M41S family and comparatively better stability of materials, has been widely studied because of its one dimentional ordered hexagonal array of pores [15]. For the first time, titanium containing MCM-41 materials were reported by a research group of Corma. et. al in 1994 [10,11] and since then, this material has been utilized as catalyst for various reactions, such as the oxidation of oelfins [11], epoxidation of allyl chloride[16], unsaturated alcohols [17] and plant oils [18], isomerization of [19], photocatalysis [20], limonene oxidation [21] and the oxidation of organic sulphide to sulfone [22]. Corma et al. [23] has found that TiMCM-41 materials have shown much lower activity for the oxidation of small organic molecules than the TS-1 and Ti(Al)-beta zeolites due to the lower hydrophobic nature of the catalyst which allow the water molecules to be adsorbed on the catalytic sites and thus poisoning the catalytic active sites. To avoid catalyst poisoning the hydrophobic character should be improved because hydrophilic-hydrophobic property of the catalyst plays a vital role for liquid phase oxidations [24]. Kwang-Min Choi et al. [25] reported the synthesis of Ti containing MCM-41 materials from molecular precursor tetrakis (tris-tert-butoxysiloxy) titanium as a titanium source. Highly active and selective titanium containing MCM-41 materials were synthesized through a grafting route using titanium (IV) acetylacetonate as titanium source [26]. Ti MCM-41 catalyst suffered leaching of titanium ions in the presence of H_2O_2, resulting in deactivation of the catalyst. To prevent the deactivation of catalyst, enhancement of hydrophobicity of the catalyst is a vital factor to improve the catalytic activity of Ti-substituted mesoporous molecular sieves in the liquid phase oxidation with aqueous solution of H_2O_2. Hui Zhou et al [27] reported the synthesis of defectless organo-titanosilicate with increased hydrophobic character at room temperature.

The hydrophobicity of TiMCM-41 materials can be improved by two general approaches, one is the post synthetic silylation treatment and other is the direct the one pot (co-condensation) method. Corma et al. [28] reported the synthesis of one step highly active and selective methylated silicones functionalized Ti containing MCM-41 materials catalyst for cyclohexene epoxidation reactions under hydrothermal conditions. One problem associated with the use of high hydrothermal temperature is that it

produced anatase phase of TiO_2 and the problem could be reduced by carrying out the reaction at lower temperature. Kaifeng Lin et al. [29] reported dilute solution route for the synthesis of methyl functionalized Ti incorporated MCM-41 materials at room temperature.

In this report, synthesis of methyl functionalized TiMCM-41 catalyst at room temeprature using NH_3 base avoiding of NaOH has been reported. NaOH has been found to be having harmful effect in this system. Four catalysts with four different methyl loadings have been prepared and their catalytic activity has been tested for the epoxidation of cyclohexene using aqueous hydrogen peroxide as an oxidant. As the oxidant, H_2O_2 does not cause environment pollution, is of low cost and produces only water, besides the major product under mild reaction conditions. Due to good oxidative properties, H_2O_2 has found applications in many processes, displacing other chemical oxidants which are associated with the formation of wastes [18].

2. Experimental

2.1 Materials:

Cetyltrimethylammoniumbromide (CTAB, RANKEM), tetraethylorthosilicate (TEOS, Merck), ammonium hydroxide (25 %), absolute alcohol, diethyl ether (Merck), methyltriethoxysilane (MTES, Sigma Aldrich), titanium isopropoxide (TIP, Merch), Cyclohexene (SRL, India), hydrogen peroxide (30 %, Merck), acetonitrile (AR, Merck). All the chemicals were of analytical grade and used without further purification.

2.2 Synthesis of methylated TiMCM-41

MCM-41 materials in silicon system (parent) and titanium silicon system were synthesized according to the literature [30]. The functionalized TiMCM-41 materials were synthesized by adding 0.5 g of CTAB (cetyltrimethylammoniumbromide) to a solution of 96 mL of deionized water. When the solution turned clear, 34 mL of ethanol (absolute alcohol) along with 10 mL of ammonia (25 %) were added to the

solution and continued stirring for 5 min at room temperature. 2.0 mL of TEOS along with calculated amount of MTES and titanium isopropoxide (TIP) were added into to the solution under stirring. Stirring was continued for 3 h at room temperature after completion of reaction. The solid product were collected by filtration and dried at room temperature for 12 h. The surfactant was removed from the materials by solvent extraction method [10]. The methyl-functionalized Ti-MCM-41 materials were treated with a solution of 1M HCl in diethylether (solid: liquid =1 g: 100 mL) for 24 h at room temperature [29]. The solids were separated by filtration, washed with excess of ethanol, and again dried at 60 ^{O}C. By adopting the above mentioned method, four different methyl functionalized TiMCM-41 samples with 5, 10, 15 and 20 mol % of MTES w.r.to TEOS in the starting gel were prepared and designated as 5MeTiM-1, 10MeTiM-1, 15MeTiM-1 and 20MeTiM-1 respectively.

2.3 Characterization:

Low angle powder X-ray diffraction patterns of the synthesized materials were recorded on Bruker D8 diffractometer, Ni- filtered CuK_{α} radiation of wavelength 1.5404 A$^{\circ}$, between 0.5 and 10 (2θ) with step size 0.02 . Characterization of morphology of the synthesized materials was performed with scanning electron microscope (SEM) and transmission electron microscope (TEM) .The materials for TEM studies were prepared by first sonicating ~2 mg of 10MeTiM-1 in 10 mL of ethanol for at least 30 min. One drop of this dispersion was carefully deposited on a carbon coated copper grid (200 mesh). The grid was allowed to dry at room temperature overnight before TEM analysis. SEM micrographs of the synthesis samples were obtained on JEOL-JSM-6360 instrument while the TEM images were obtained on a JEM -2100 instrument. FT-IR spectroscopy analysis was done using Shimadzu IR Affinity -1 and by using KBr pellets. Diffuse reflectance UV-vis spectra were recorded in the range of 200–800 nm with Hitachi U-4100 spectrometer equipped with a diffuse reflectance attachment, using $BaSO_4$ as the reference. Thermogravimetry analysis was carried by using Mettler Toledo TGA/DSC STAR^{e} system in the presence of nitrogen atmosphere with a flow rate of 50 mL/min in the temperature range of 25 ^{O}C – 700 ^{O}C. The N_2 adsorption-desorption was performed at 77 K by using Micromeritics Tristar 3000 porosity

meter. Prior to measurement the samples were degased at 150 ^{O}C for 12 h. Ti concentration in the materials was calculated by using energy dispersive X ray spectroscopy and also determined with Thermo Scientific 7000 series of ICP-OES instrument.

2.4 Catalytic Reactions

The catalytic oxidation of cyclohexene was carried out in 25 mL two-necked round bottom flask equipped with a refux condenser. In a typical reaction, 50 mg of catalyst was mixed with 5 mL of solvent (acetonitrile), 1 mL of cyclohexene (10 mmol) and 20 mmol of H_2O_2 (30 % aqueous) as oxidant and stirred magnetically upto 7 h at 333 K uder atmospheric pressure. For the recyclability tests, the catalyst was filtered off, washed twice with fresh solvent (ethanol), heated at 80 ^{O}C for overnight at 12 h, cooled down to room temperature and reused under the same reaction conditions. The catalyst was separated from product mixture in each case by centrifugation and the products were analyzed by Perkin Elmer Clarus 500 gas chromatograph equipped with Elite-1 series of capillary column using flame ionization detector (FID).

Conversion and selectivity were calculated using following relations

Conversion (%) = 100 × $[C_6H_{10}]_0 — [C_6H_{10}] / [C_6H_{10}]_0$

$[C_6H_{10}]_0$ = Initial concentration of cyclohexene

$[C_6H_{10}]_t$ = Concentration of cyclohexene at time t

Selectivity (%) = 100 x moles of individual product / moles of total products

3. Result and discussion

3.1 Characterization

3.1.1 XRD analysis:

Figure 2 shows the XRD pattern of calcined SiMCM-41 material which is in good agreement with that reported for the 2D hexagonal MCM-41 materials [30]. It is evident that the parent MCM-41 sample

exhibits reflections corresponding to the (100), (110) and (200) planes, indicating an ordered 2D-hexagonal (p6mm) arrangement of channels.

Comparing the d_{110} value of parent and organically modified TiMCM-41 sample, the functionalized samples exhibit smaller unit parameter as evident from the Fig. 2 and the shift in 2θ value to a higher angle is observed. This could be attributable to the repulsive interaction between organic groups and inorganic-organic double layer [31, 32]. The XRD patterns of the inorganic and directly organically functionalized TiMCM-41 (up to 10 mol % of methyl w.r.t TEOS) exhibit d_{100}, d_{110} and d_{200} reflections, indicating a well ordered 2d-hexagonal (p^6mn) arrangement of channels as shown in the Fig. 2. However, the higher order reflection is missing when methyl loading exceeds 15 mol %, resulting in the formation of less order mesoporous materials.

Hexagonal mesoporous structure of the MCM-41 material was found to maintain after metal incorporation. However, a shift to higher 2 theta values is observed after metal loading.

3.1.2 FTIR analysis:

FTIR spectra of the sample are shown in Fig. 3. For all samples, the broad band at ca. 3468 cm^{-1} is ascribed to water. The weak band at 1630 cm^{-1} corresponds to the bending mode of water. The broad band at ca. 1084 cm^{-1} with a shoulder peak at 1234 cm^{-1}, and the band at 810 cm^{-1} are attributed to Si-O-Si asymmetric stretching and Si-O-Si bending vibration respectively. The absorption peak at 960 cm^{-1} that is observed in the pure silica MCM-41 sample is usually assigned to the stretching vibrations of ν_{as} (Si-OH) or ν_{as} (Si-O-M) (M=metal) vibration for heterogeneous metal loaded samples [33]. According to Boccuti et al. [34], this absorption band at ca. 960 cm^{-1} can be assigned to a stretching mode of (SiO_4) unit bonded to a Ti (IV) ion for (O_3SiO-Ti). So this band can be considered as a proof of titanium substitution in the frame work of mesoporous materials. Although parent MCM-41 material also shows this band at 960 cm^{-1}, the band for parent MCM-41 is weak and also for Ti substitution on mesoporous materials, the intensity of this band increases with titanium incorporation in the framework [35].

3.1.3 Thermogravimetric analysis:

The TGA plots of CTAB are shown in the Fig. 4 and it shows two step of weight loss in the temperature ranges of 200 ^{O}C-300 ^{O}C and 300 ^{O}C-540 ^{O}C. The uncalcined MCM-41 sample shows three steps of weight loss in the temperature ranges of 25 ^{O}C-150 ^{O}C, 150 ^{O}C-200 ^{O}C and 200 ^{O}C-540 ^{O}C. The TGA curves of 5MeTiM-1 (Si/Ti 40), 10MeTiM-1 (Si/Ti 40), 15MeTiM-1 (Si/Ti 40) and 20MeTiM-1 (Si/Ti 40) are shown in the Fig. 4.

All the samples show five steps of degradation in the temperature ranges 25 ^{O}C-150 ^{O}C, 150 ^{O}C-200 ^{O}C, 200 ^{O}C-300 ^{O}C, 300 ^{O}C-540 ^{O}C and 540 ^{O}C-600 ^{O}C. As observed from the Table 2 mass percentage loss was maximum for as synthesized uncalcined MCM-41 material and for methyl functionalized TiMCM-41 materials the weight loss % decreases gradually from 51.46 % to 31.9 % when MTES loading was increased from 5 % to 20 % w.r.t TEOS in the gel mixture. However, the loss was found to decrease with methyl loading may be due to increase in hydrophobic character of the catalyst [37]. The samples were thermally stable, however, this stability was found to decrease with increasing methyl loading.

3.1.4 Diffuse reflectance UV Visible spectroscopy analysis:

DR UV-Visible spectroscopy is vital tool for determining the co-ordination environment of the metal ion in the framework of mesoporous MCM-41 materials. The UV-Visible DRS spectra of all samples (Fig. 5) show an intense broad band centred at 230-240 nm along with less intense shoulder peak at ~270 nm. The titanium species in the samples may be isolated and tetrahedrally coordinated inside the framework of MCM-41 as indicated by the broad absorption band appeared at around 221 nm [46]. This band can be interpreted as a ligand to metal charge transfer transition from oxygen to isolated tetrahedral titanium (IV). When the coordination number is more than four, such as bonding with water molecules beside the metal coordination sphere, the absorption band will be shifted to longer wavelengths or lower energies. The absorption band at a higher wavelength (~270 nm) is probably corresponds to partially polymerized

titanium species (five- or six- coordinated) [48]. From the graph it is revealed that at high loading of methyl group onto TiMCM-41 materials shifted the absorption band at~ 221 nm (for tetra-coordinated Ti^{4+} ion) to a higher wavelength, indicating the formation of extra framework penta or hexa co-ordinated Ti ion/ which may be an indication that there is a possibility of titanium forming in either a disordered tetrahedral environment or in octahedral coordination spheres.

3.1.5 N_2 adsorption-desorption isotherm analysis.

N_2 adsorption-desorption isotherms of calcined MCM-41 and organo modified TiMCM-41 samples are shown in figure 6. All the samples give typical IV type isotherms with H^3 hysteresis loop and a sharp inflection at $p/p_o > 0.3$, indicate typical mesoporous solid [38]. This is characterized of capillary condensation, which points to the uniformity of meso pore sizes distribution.

The pore size of functionalized MCM-41 material is higher than the parent MCM-41material, which could be attributed to the higher amount of methyl groups in the former materials. The BET surface area of the organic modified TiMCM-41 materials have increased as the methyl loading increases up to (10 mol %) methyl and beyond that loading, BET surface area decreases gradually.

It is worth noting that the 10MeTiM-1sample has highest BET surface area than the parent and other high loading methyl functionalized TiMCM-41 materials. This is due to the small particle size of the 10MeTiM-1 material as evident from the TEM image of 10MeTiM-1 (Fig. 7 B).

Surface area (m^2/g), pore volume (cm^3/g) and pore size (nm) are calculated from N_2 adsorption measurement.

3.1.5 Scanning electron micrograph (SEM) and Transmission electron micrograph analysis (TEM).

The SEM images of parent MCM-41 are shown in the Fig. 7 (A). From the figure, it is observed that the particles are nearly spherical in shape with size ranges from 0.3-0.5 μm. The TEM image of 10MeTiM

sample shows the existence of regular hexagonal arrays and parallel one dimensional mesoporous channels within these particles. From the TEM image the size of the particles are calculated and found in the range of 108.2 to 141.4 nm. The SAED pattern of TEM image has shown some circular ring indicating the amorphous nature of the materials.

Titanium concentrations in the sample are calculated from EDX and result shows 1.5 mmol / g of titanium incorporation. This is further confirmed by ICP-OES measurement which shows 1.4 mmol / g of Ti loading.

The energy dispersive X-ray (EDX) elemental mapping analysis demonstrates uniform distribution of elements of Ti and O in the modified 10MeTiM-1, as shown in Fig. 7 (D).

3.2 Catalytic activity

3.2.1 Effect of methyl loading onto MCM-41(Si/Ti 40) on cyclohexene oxidation.

The effect of methyl loading onto TiMCM-41 materials on cyclohexene oxidation reaction was studied in the presence of H_2O_2 as oxidant for a period of 7 h at 60 ^{O}C in acetonitrile (CH_3CN) solvent with cyclohexene: H_2O_2 molar ratio of 1:2. The results are shown in the Fig. 8 (A). The maximum conversion (38.8 %) was obtained for the catalyst10MeTiM with maximum epoxide selectivity of (68.8 %). From the Fig. 8 (A) it is observed that as methyl loading in TiMCM-41 increases the conversion at first increased up to 10

% methyl loading after that conversion and selectivity both decreased. This is probably due to the hydrophobic nature and change in surface area of the materials. Observing the weight loss in the temperature range 25-150 ^{O}C in table 2 it is observed that the hydrophobicity of the materials increased with increase of methyl loading, but the surface area and pore volume of the materials decreased with the

increase of methyl loading and the maximum surface area was found to be at 10 % of methyl loading. Therefore, all other cyclohexene oxidation reaction was carried out by using this catalyst.

3.2.2 Effect of cyclohexene: H_2O_2 molar ratio

The effect of cyclohexene: H_2O_2 molar ratio on the conversion of cyclohexene and selectivity towards cyclohexene epoxide after 7 h at 60 ^{O}C with 10MeTiM-1 of catalyst amount 0.05 g with respect to cyclohexene was studied. From the Fig. 8 (B), it is observed that as the molar ratio of cyclohexene: H_2O_2 decreased from 1 to 0.5, the conversion and selectivity both increased. However, when molar ratio was increased to 2:1 both conversion and selectivity both decreased. The highest conversion and selectivity are obtained for cyclohexene: H_2O_2 molar ratios of 1:2 as more oxidant are available with respect to substrate.

3.2.3 Effect of temperature:

The cyclohexene conversion initially increased with the rise of temperature from 25 to 60 ^{O}C and then decreased slightly at a higher temperature (80 ^{O}C). The increase of reaction rate with temperature was expected according to the Arhenius equation .The low conversion and selectivity at 80 ^{O}C might be due to rapid decomposition of hydrogen peroxide at this temperature. In any case, temperature appeared to support selectivity toward cyclohexene epoxide unfavourably possibly due to further oxidation of the products.

3.3.4 Effect of catalyst amount:

The effect of catalyst amount on conversion and selectivity to cyclohexane epoxide was investigated by taking different amounts of the catalyst (15 to 100 mg) with respect to reactant at 333 K with cyclohexene: H_2O_2 molar ratio of 1:2 using acetonitrile as solvent. From the Fig. 8 (D) it is observed that the maximum cyclohexene conversion was obtained when 50 mg of catalyst was used with respect to substrate. The reason of the maximum conversion is due to large number of active site available in the

framework of the materials which enhance the rate of the reaction. At first the selectivity for epoxide increased with increase of catalyst amount attaining highest for 25 mg of catalyst and after that selectivity gradually decreased which may be due to the opening of epoxide ring or further oxidation of the product.

3.3.5 Effect of solvent

While glancing through the literature, it was found that solvent plays a crucial role in liquid phase reaction as it alters the reaction kinetic as well as product selectivity [41]. In general, aprotic solvent is more effective than protic solvent as it increases the substrate concentration around the catalyst active sites. Highly polar aprotic solvent will increase the substrate concentration, which favours the catalytic reaction [42]. In the present study four different aprotic solvents (DCM, acetonitrile, DMF and chloroform) with different polarities were used. From the Fig. 9 (B), it is observed that acetonitrile gave maximum cyclohexene conversion with highest epoxide selectivity. Among the solvents used acetonitrile had the highest dipole moment (3.92 D)

3.3.6 Effect of time

From Fig. 9 (A), it is observed that the cyclohexene conversion increased from 9.1 % to 38.8 % as the reaction time increased from 1 h to7 h. The selectivity to epoxide decreased gradually with time is due to the hydrolysis of the epoxide product to cyclohexane diol. The optimum time for the reaction was found to be 7 h.

Reaction mechanism:

Ti (IV) species considered to be the catalytic active sites of methyl functionalized TiMCM-41 materials in the oxidation of cyclohexene to cyclohexene epoxide should involve the following steps [43, 44]. Three main reaction steps should be involved, as shown in the Fig. 15 Ti (IV) species on the surface react with

H_2O_2 to form titanium hydroperoxide, which further react with cyclohexene molecules to form cyclohexene epoxide in a concerted manner.

4. Conlcusions:

The methyl functionalized Ti MCM-41 materials are successfully synthesized according to the literautue [9]. Four numbers of catalyst with different methyl loading are synthesised by using NH_3 as a base avoid of NaOH at room temperature after a period of 3 h. Here, we avoided the use of NaOH as it was used by many researchers for the synthesis of pure MCM-41 materials. It is known, however, that there is a detrimental effect of the use of alkali metal ions in the catalytic properties of metal incorporated silicious molecular sieves.

TEM and SEM results confirmed the formation of ordered hexagonal arrays with one dimentional parallel channels and successful incorporation of titanium and methyl group. Characterization results also revealed the existence of two types of titanium ions, one is tetra-coordinated Ti ions which are present in large quantity along with small amount of penta or hexa-coordinated titanium ions. The N_2 adsorptin desorption isotherm shows that the position of hysteris loop slightly shifted to the higher relative pressure range indicate the existance of particle of large pore diameter. In the epoxydation reaction, 10MeTiM-1 shows the highest cyclohexene conversion and epoxide selectivity.

The improved catalytic performance of 10MeTiM-1 is recognized to the combined effect of shorter mesoporous channels, small particle size and of hydrophobicity of the catalyst produced after methyl functionalization. The cyclohexene conversion and epoxide selectivity both gradually decrease with high methyl loading possibly due to the shrinkage of pore volume.

Acknowledgements

The authors are thankful to UGC-BSR, New Delhi for financial support. The authors would also like to thank IASST DST Boragaon, SAIF NEHU Shillong and Department of Chemistry, Gauhati University

for providing the available research facilities that were of immensely helpful in carrying out the present work.

References

1. L. Fan, G. Qin, & S. Cao, Arab J Sci Eng. 40 (2015) Issue 10 2861-2866.
2. M. Taramasso, G. Perego, B. Notari, US Patent. 4410501 (1983).
3. A.Tuel, Zeolite 15 (1995) 236.
4. D. P. Serrano, H. X. Li, M. E. Davis, Chem.Commun. (1992) 745.
5. A. Corma, M. A. Camblor, P. Esteve, A. Martinez, J. Perez-Pariente, J. Catal. 145 (1994) 151.
6. T. Tatsumi, N. Jappar, J. Phys. Chem. B 102 (1998) 7126.
7. A. Corma, P. Esteve, A. Martinez, J.Catal. 161 (1996) 11.
8. B. Notari, Adv. Catal. 41 (1996) 11.
9. P. Ratnasamy, D. Srinivas, H. Knozinger, Adv. Catal. 48 (2004) 1.
10. P. T. Tanev, M. Chibwe, T. J. Pinnavaia, Nature. 368 (1994) 321.
11. A. Corma, M. T. Navarro, J. Perez-Pariente, Chem-Commun. (1994) 147.
12. T. Blasco, A. Corma, M. T. Navarro, J. Perez-Pariente, J. Catal. 156 (1995) 65.
13. O. Franke, J. Rathousky, G. Schulz-Ekloff, J. Starek, A. Zukal, Stud. Surf. Catal. 84 (1994) 77.
14. T. Maschmeyer, F. Rey, G. Sankar, J. M. Thomas, Nature. 378 (1995) 159.
15. P. Selvan, S. K. Bhatia, C. G. Sonwane, Ind. Eng. Chem.Res. 40 (2001) 3237.
16. A. Wroblewska, E. Milchert, Chem. Pap. 56 (2002) 150.
17. C. Berlini, M. Guidotti, G. Moretti, R. Psaro, N. Ravasio, Ctal. Today. 60 (2000) 219.
18. L. A. Rios, P. Weckes, H. Schuster, W. F. Hoelderich, J.catal. 232 (2005) 19.
19. T. N. Siva, J.M. Lopes, F.R. Ribeiro, M.R. Carrott, P.C. Galacho, M.J. Sousa, P. Carrott, Reaction Kinetics and Catalysis Letters. 77 (1) (2002) 83-90.
20. N.B. Lihitkar, M. K. Abyaneh, V. Samuel, R. Pasricha, S.W. Gossavi, S.K. Kulkarni, J. Colloid Interface Sci. 314 (1) (2007) 310-316.
21. M. Guidotti, R. Psaro, I. B. Gener, E. Gavrilova, Chem.Eng.technol. 34 (2011) 1924.
22. A. Corma, M. Iglesias, F.Sanchez, Catal. Lett. 39 (1996) 153.

23. T. Blasco, A. Corma, M.T. Navarro, J. Perez-Pariente, J.Catal. 156 (1995) 65.

24. A. Corma, P. Esteve, A. Martinez, J. Catal. 161 (1996) 11.

25. K. M. Choi, T. Yokoi, T. Tatsumi, K. Kuruda, J.Mater.Chem.A. 1 (2013) 2485-2494.

26. M. Fukuda, N. Tsunoji, Y. Yagenji, Y. Ide, Shinjiro, M. Sadakane, T. Sano, J. Name. 00 (2013) 1-3.

27. H. Zhou, L. Xiao, X. Liu, S. Li, H. Kobayashi, X. Zheng, Chem Commun. 48 (2012) 6954-6956.

28. A. Corma, J.L. Jorda, M. T. Navarro, F. Rey, Chem. Commun. 1998, 1899-1900.

29. L. Kaifeng, P. P. Paolo, H. Kristof, L. Duoduo, T. V. Gustaaf, J. A. Pierre, J. Catal. 263 (2009) 75-82.

30. H. I. M. Ortiz, Y. P. Mercado, J. A. M. Silva, Y. O. Maldonado, G. Castruita, L. A. G. Cerda, Ceram. Int. 40 (2014) 9701-9707.

31. J. Aguado, J. M. Arsuaga, A. Arencibia, M. Lindo, V. Gascon, J. Hazard. Mater. 163 (2009) 213–221.

32. S. Rana, S. Mallick, and K. M. Parida, Ing & Eng. Chem. Res. 50 (2011) 2055-2064.

33. H. Faghihian, M. Naghavi, Sep. Sci. Technol. 49 (2014) 214–220.

34. B. Kalita, P. Phukan and A. K. Talukdar, Catal. Sci. Technol. 2 (2012) 2341–2350.

35. M. R. Prasad, G. Madhavi, J. Porous Matter. 13 (2006) 81-94.

36. M. Rzepkowska, A. Wroblewska and G. Lewandowski, Chem. Pap. 58 (2004) 324-329.

37. J. Bu and H. K. Rhee, Catalysis Letters. 65 (2000) 141-145.

38. T.W. kim, P. W. Chung, and V. S. Y. Lin, Chem. Matter. 22 (2010) 5093-5104.

39. L. Kaifeng, P. P. Paolo, H. Kristof, L. Duoduo, T. V. Gustaaf, J. A. Pierre, J. Catal. 263 (2009) 75-82.

40. M. Fukuda, N. Tsunoji,Y. Yagenji, Y. Ide, S. Hayakawa, M. Sadakane, T. Sano, J. Name. 00 (2013) 1-3.

41. W. C. Zhan, Y. L. Guo, Y. Q. Wang, X. H. Liu, Y. Guo, Y. S. Wang, Z. G. Zhan and G. Z. Lu, J. Phys. Chem. B. 111 (2007) 12103-12110.

42. D. Chen, N. Li, P. Sun and Y. Kong, Chin. J. Catal. 30 (2009) 643-648.

43. W. Zhan, Y. Guo, Y. Wang, X. Liu, Y. Guo, Y. Wang, Z. Zhang, and G. Lu, J. Phys. Chem. B. 111 (2007) 12103-12110.

44. H. Wang, W. Qian, J. Chen, Y. Wu, X. Xu, J. Wang, and Y. Kong, RSC Adv. 4 (2014) 50832

45. C. Peng, X. H. Lu, X. T. Mab, Y. Shen, C. C. Weia, J. Hea, D. Zhou, Q. H. Xia, J. Mol. Catal. A Chem 423 (2016) 393–399.

46. M. Bandyopadhyay, A. Birkner, M. W. E. van den Berg, K. V. Klementiev, W. Schmidt, W. Gru¨nert, H. Gies. Chem. Mater. 17 (2005) 3820-3829.

47. N. Igarashi, S. Kidani, R. Ahemaito, K. Hashimoto, T. Tatsumi, Microporous and Mesoporous Mater 81 (2005) 97–105.

48. N.Thanabodeekij, W. Tanglumlert, E.Gulari, S. Wongkasemjit. Appl. Organometal. Chem. 19 (2005) 1047–1054

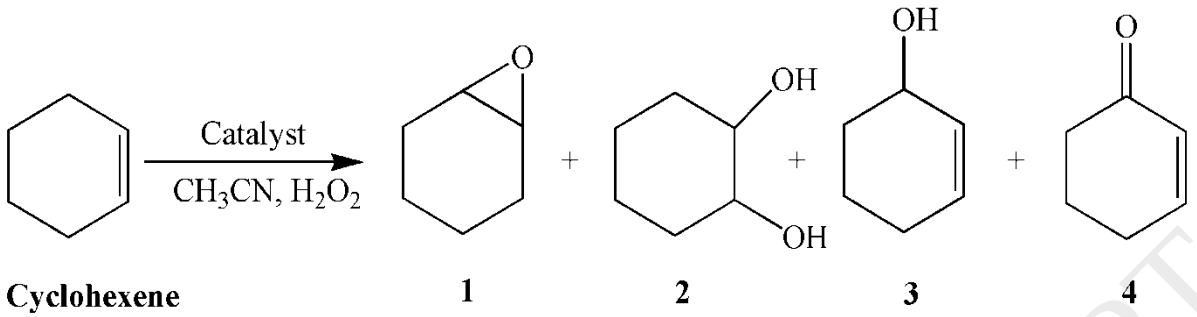

1 = Cyclohexane epoxide, 2 = Cyclohexane diol, 3 = 2-Cyclohexene-1-ol

4 = 2-Cyclohexene-1-one

Fig. 1 Reaction scheme for oxidation of Cyclohexene

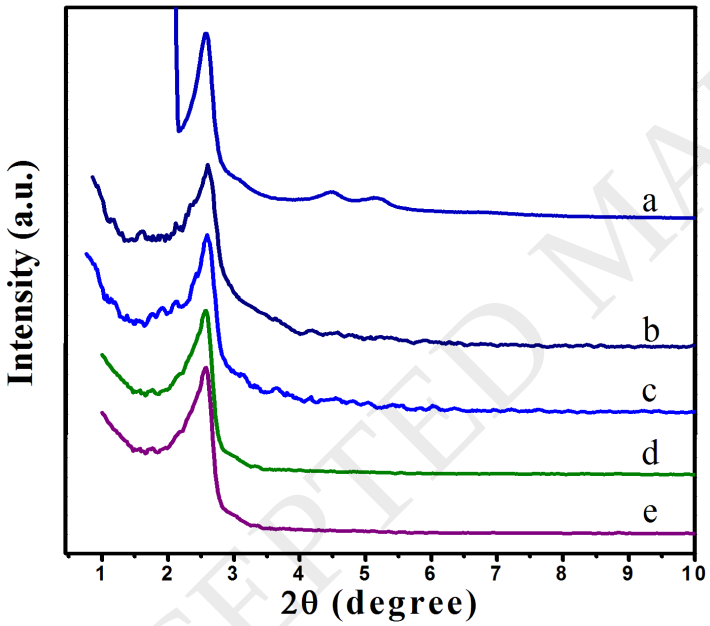

Fig. 2 XRD pattern of parent MCM-41 (a) 10MeTM-1 (b) TiMCM-41 (Si/Ti 40) (c) TiMCM-41 (Si/Ti 60) (d) TiMCM-41 (Si/Ti 80)

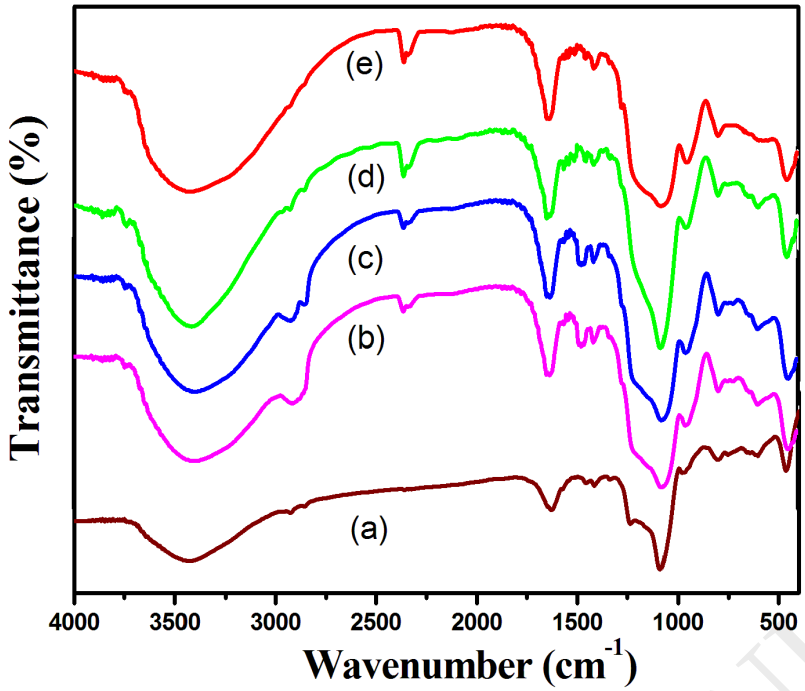

Fig. 3 FT-IR spectra of (a) parent MCM-41, (b) 5MeTM-1, (c) 10MeTiM-1, (d) 15MeTiM-1 and (e) 20 MeTiM-1

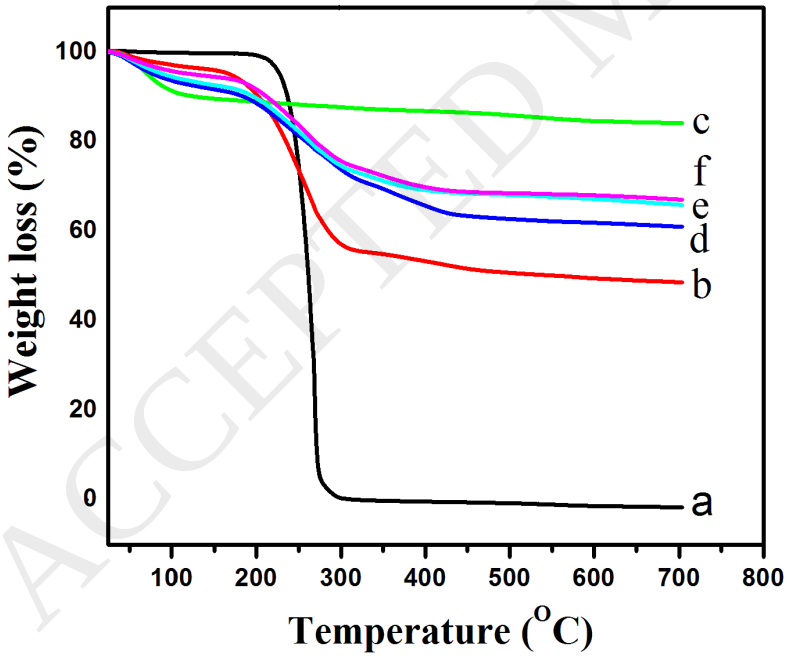

Fig. 4 TGA curve of CTAB (a) uncalcined parent MCM-41(b) 5MeTiM-1 (c) 10MeTM-1 (d) 15MeTiM-1 (e) 20MeTM-1

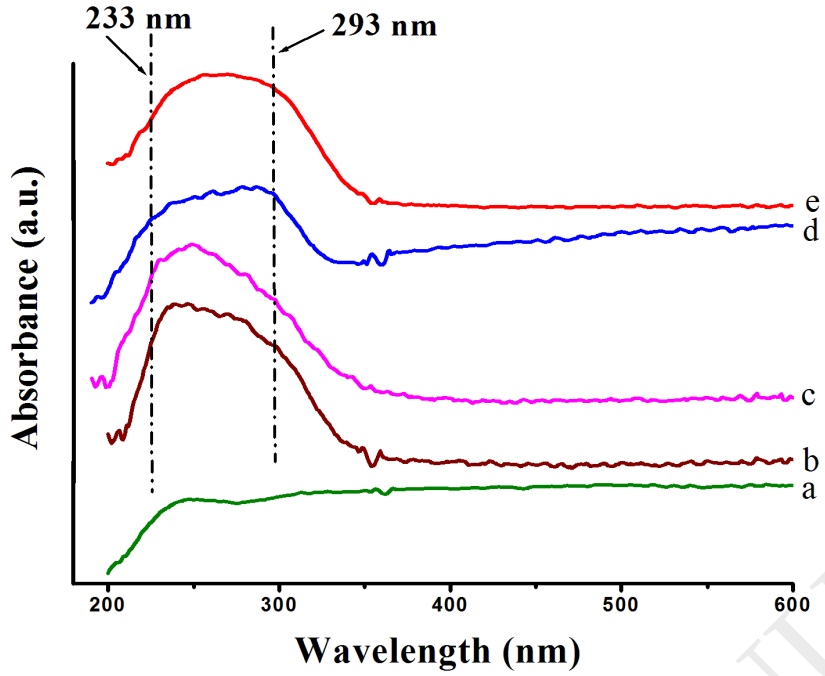

Fig. 5 DR UV Visible spectra of calcined parent MCM-41 (a) 5MeTiM-1 (b) 10MeTiM-1 (c) 15MeTiM-1 (d) 20MeTiM-1 (e)

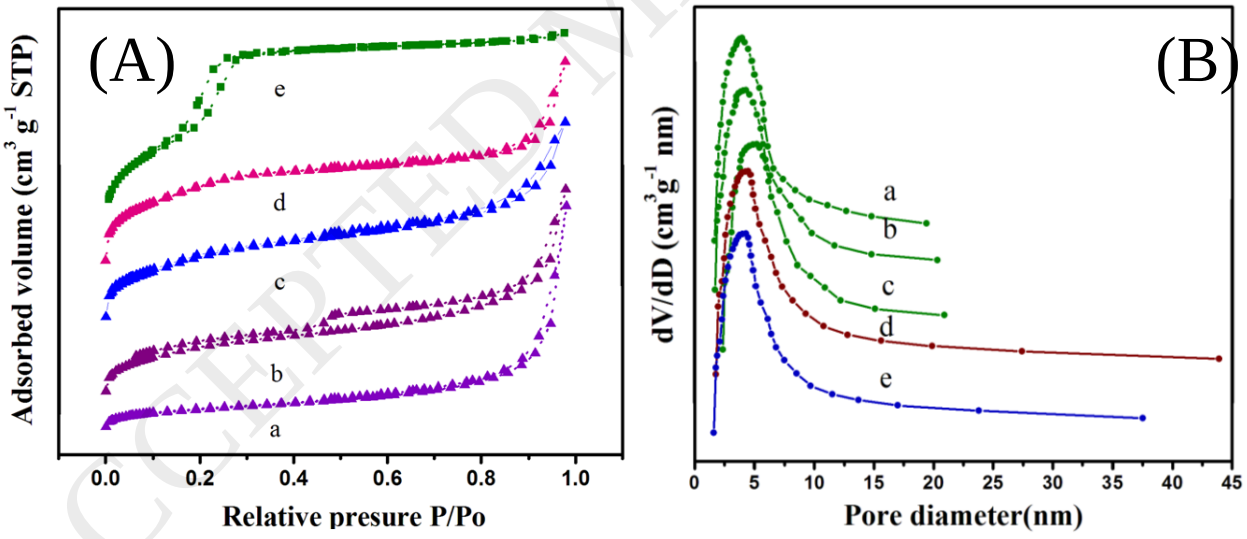

Fig. 6 (A) N_2 adsorption-desorption isotherm of 5MeTiM-1 (a) 10MeTiM-1 (b) 15MeTiM-1 (c) 20MeTiM-1 (d) parent MCM-41 (e) (B) Pore size distribution curve of parent MCM-41 (a) and modified TiMCM-41 (b-e)

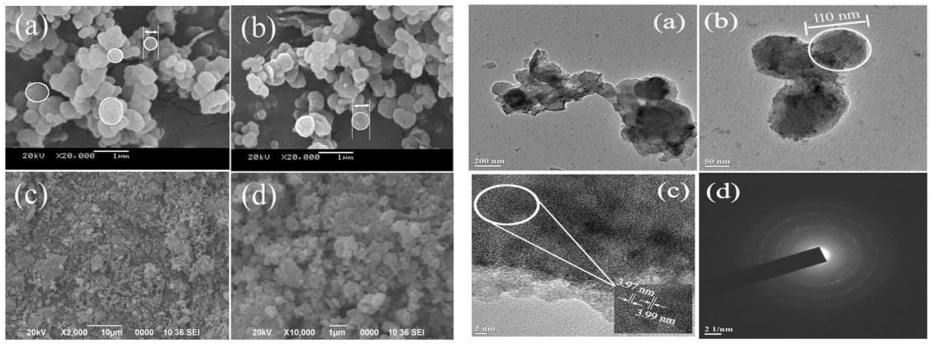

(A) (B)

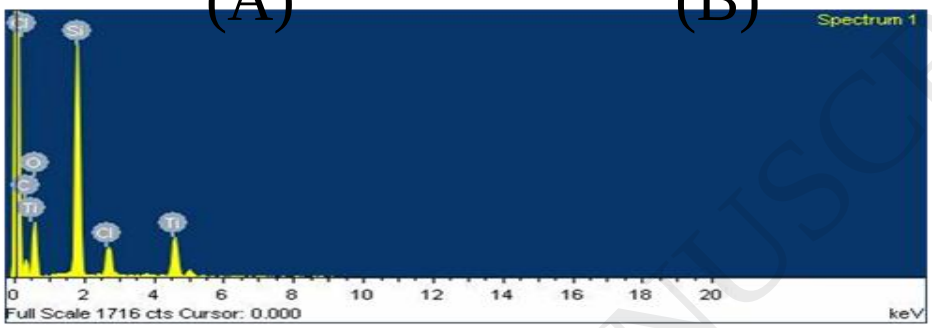

(C)

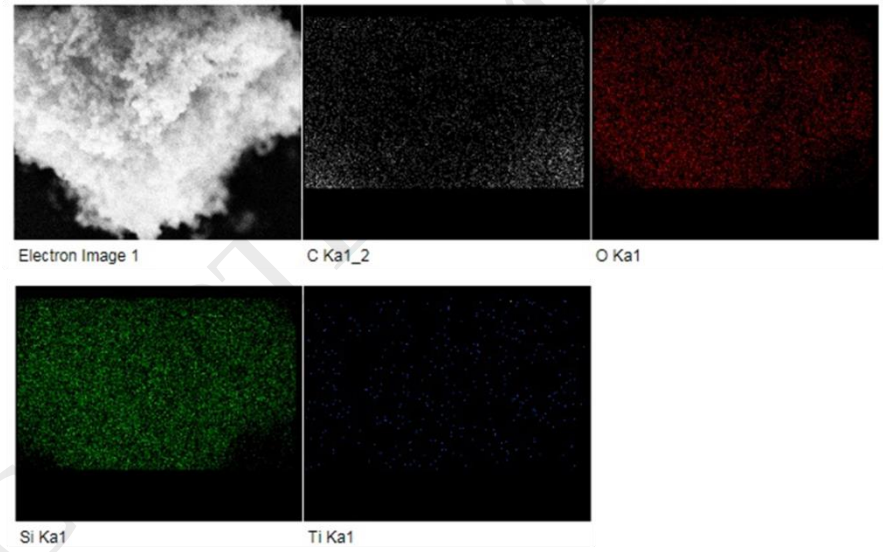

(D)

Fig. 7 (A) SEM image of parent MCM-41 (a, b) and modified 10MeTiM-1 (c, d)

(B) TEM image of modified 10MeTiM-1 (a-c) and SAED pattern of TEM of 10MeTiM-1(d)

(C) EDX spectra of modified 10MeTiM-1

(D) EDX mapping of 10MeTiM-1

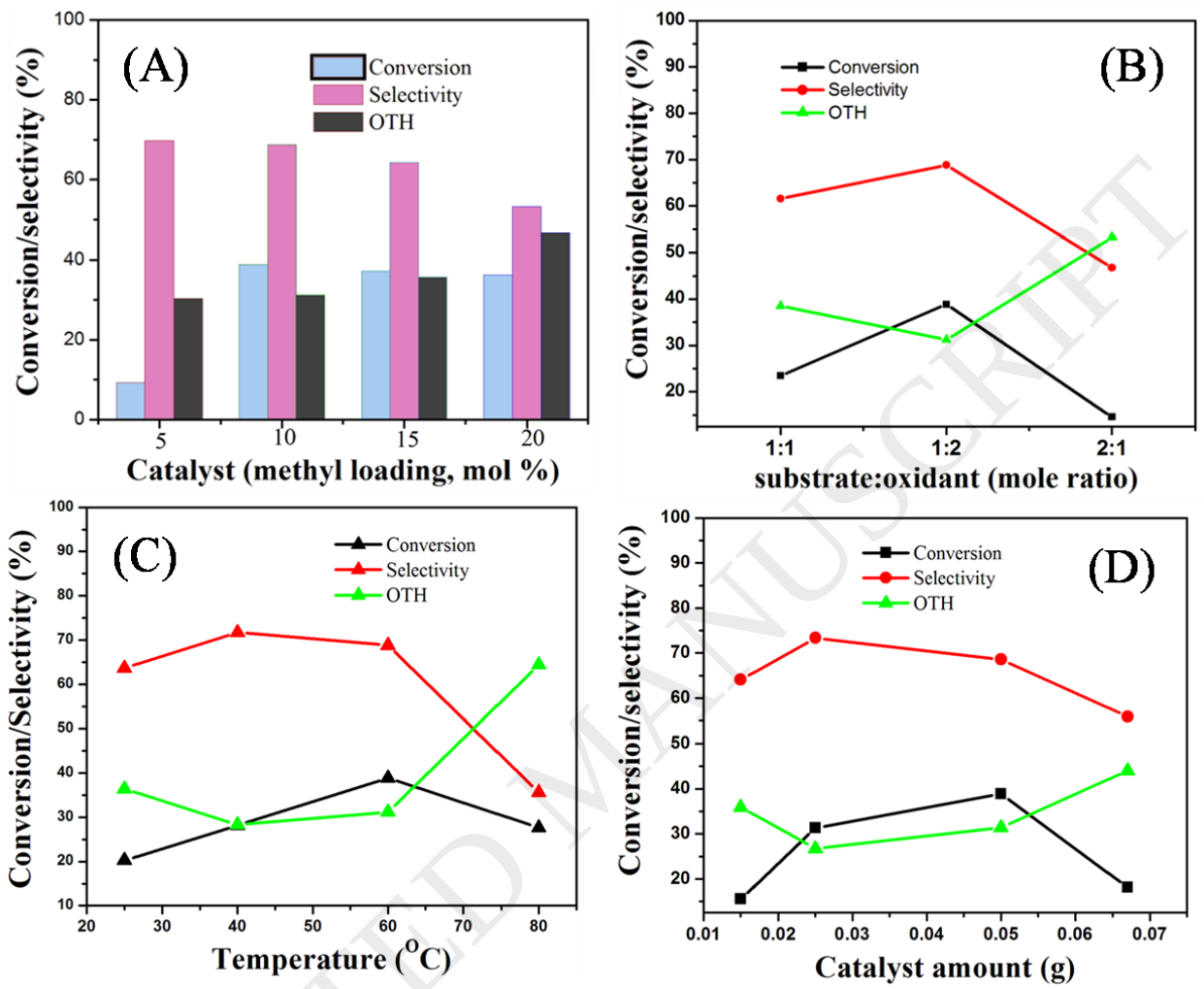

Fig. **8 (A)** The effect of methyl loading (mmol) (B) effect of substrate and oxidant mole ratio (C) effect of temperature (^{O}C) (D) effect of catalyst amount (g) on cyclohexene conversion. Reaction conditions: cyclohexene = 1 mL (10 mmol), H_2O_2 = 20 mmol, temperature = 60 ^{O}C, time = 7 h, catalyst amount = 50 mg, Volume (solvent + Reactant) = 6 mL

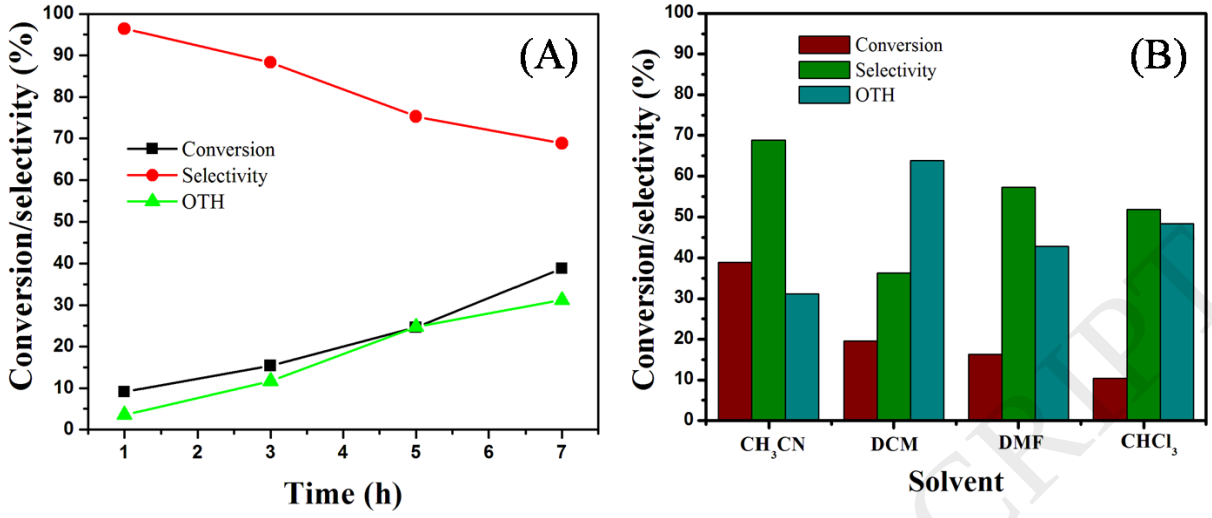

Fig. **9 (A)** Effect of time (h) (B) effect of solvent on cyclohexene conversion. Reaction conditions: Cyclohexene: H_2O_2 (1:2), temperature (60 ^{O}C), solvent 5 mL, catalyst amount 50 mg, volume (reactant + solvent) = 6 mL

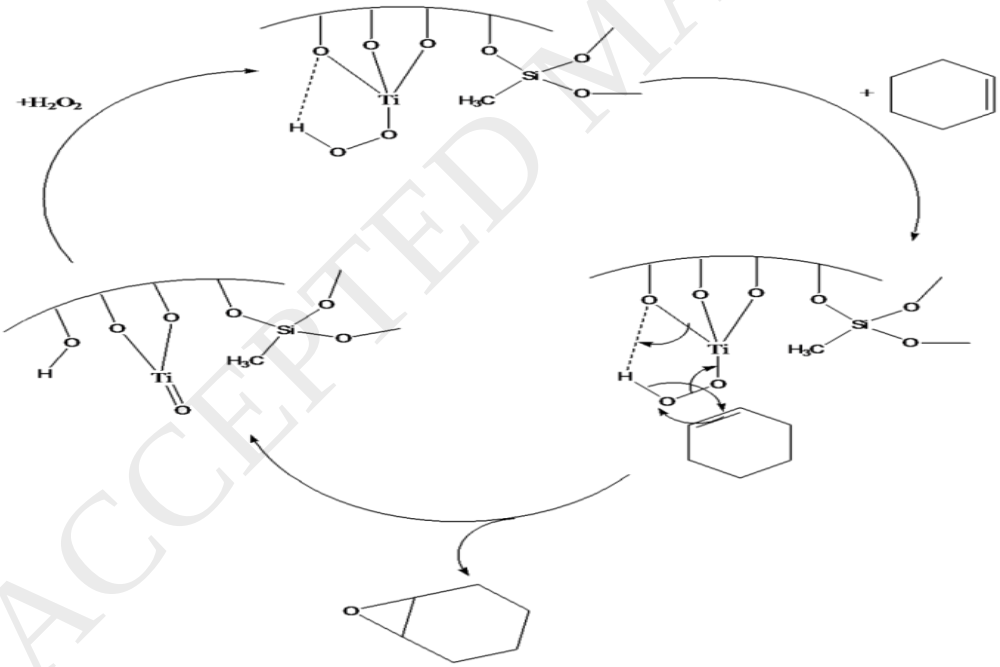

Fig. 10 Proposed reaction mechanism for the oxidation of cyclohexene to epoxide

Table 1 Designation of modified MCM-41 materials

Sample designation	Si/Ti	Methyl modification (mol % of MTES w.r.t. TEOS)
5MeTiM-1	40	5
10MeTiM-1	40	10
15MeTiM-1	40	15
20MeTiM-1	40	20

Table 2 Mass percentage loss in different sample

Catalyst	Mass percentage loss				Total mass loss
	25 ^{O}C-150 ^{O}C	150 -200 ^{O}C	200-540 ^{O}C	540-700 ^{O}C	
MCM-41	4.8	3.53	42.47	1.66	51.46
5MeTiM-1	4.1	0.83	37.75	0.16	42.68
10MeTiM-1	3.8	2.18	27.62	1.35	34.95
15MeTiM-1	3.4	1.99	26.23	1.93	33.55
20MeTiM-1	3.1	1.72	25.8	1.28	31.9

Table 3 Summary of physical properties of functionalized TiMCM-41 samples

Material	Surface area (m^2/g)	Pore volume (cm^3/g)	Pore size (nm)
MCM-41	949	0.95	2.16
5MeTiM-1	1101	0.72	3.15
10MeTiM-1	1300	0.66	3.66
15MeTiM-1	1067	0.62	6.09
20MeTiM-1	840	0.56	6.30

Table 4 Titanium concentrations calculated from EDX and ICP-OES technique

Catalyst	Experimental technique	Ti concentration (mmol/g)
10MeTiM-1 (Si/Ti 40)	EDX	1.5 mmol/g
	ICP-OES	1.4 mmol/g

Table 5 Catalytic performances in the epoxidation of cyclohexene over different catalysts[a].

Catalyst	Conversion [b] (%)	Selectivity [c] (%)
Parent MCM-41	<1.00	15.00
TiMCM-41 (40)	9.23	72.22
TiMCM-41 (60)	6.70	76.88
TiMCM-41 (80)	4.29	73.93
5 MeTiMCM-41 (40)	9.27	69.78
10 MeTiMCM-41 (40)	38.8	68.74
15 MeTiMCM-41 (40)	37.17	64.09
20 MeTiMCM-41 (40)	36.13	52.97

[a] Reaction conditions: 10 mmol of cyclohexene, 20 mmol of H_2O_2, 50 mg of catalyst, Temperature 60 ^{O}C, 7 h, [b] based on cyclohexene, [c] cyclohexene epoxide

Table 6 Catalytic performances in the epoxidation of cyclohexene over various catalysts

Catalyst	Catalyst dose (g)	Time (h)	Temperature (^{O}C)	Conversion (%)	Selectivity (%) to epoxide	References
10 MeTiM-1	0.05	7	60	38.8	68.74	**This work**
Cu(II)- CyclamSBA-16	0.05	4	80	47.3	3.6	32
TiMCM-41 LP	0.03	2	70	5.7	10.3	39
10%Me-TiMCM-41NP	0.03	30 min	60	8.4	13.4	39
Ti(acac)-MCM-41 cal	0.01	2	60	8.1	7.5	40
Ti(acac)-SBA-15	0.01	2	60	19.9	19.3	40
Anion resin supported $H_3PW_4O_{24}$	0.350	6	50	92.4	98.1	45
TiMCM-41-20Ph-2(55)[a]	0.1	3	70	72	86	47

a = Titanium incorporated MCM-41 materials functionalized with 20 mol % of PTES (phenyl triethoxysilane) w.r.t TEOS for a time period of 2 days. The number parenthesis indicates the Si/Ti mole ratio (Si/Ti 55).